THE JOURNAL OF PHYSICAL CHEMISTRY Letters

Letter

pubs.acs.org/JPCL

Angle-Dependent Ionization of Small Molecules by Time-Dependent Configuration Interaction and an Absorbing Potential

Pascal Krause and H. Bernhard Schlegel*

Wayne State University, Department of Chemistry, Detroit, Michigan 48202, United States

ABSTRACT: The angle-dependence of strong field ionization of O_2, N_2, CO_2, and CH_2O has been studied theoretically using a time-dependent configuration interaction approach with a complex absorbing potential (TDCIS-CAP). Calculation of the ionization yields as a function of the direction of polarization of the laser pulse produces three-dimensional surfaces of the angle-dependent ionization probability. These three-dimensional shapes and their variation with laser intensity can be interpreted in terms of ionization from the highest occupied molecular orbital (HOMO) and lower lying orbitals, and the Dyson orbitals for the ground and excited states of the cations.

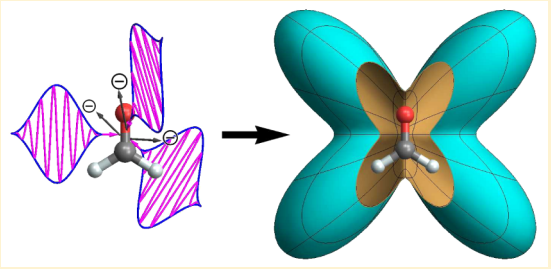

With short, intense laser pulses, it has become possible to monitor the dynamics of electrons on their natural time scale.[1−3] The angular dependence of ionization is a fundamental process in which electron dynamics plays a central role. Early work showed that the strong field ionization yield for N_2 is 4-fold greater when the molecule is aligned with the polarization of the laser than when it is oriented perpendicular.[4] Similar results were found for CO.[5] Measurement of the angular distributions of the fragments of dissociative ionization also pointed to an angular dependence of ionization.[6] The angular dependence of ionization has been measured directly for N_2, O_2, CO_2.[7,8] When a pump pulse is used to align the molecules, the ionization yield can be measured as a function of the angle between the polarization of the pump and probe pulses. The single active electron (SAE) approximation provides a good description of the angular dependence of ionization of N_2 and O_2 but has some shortcomings for CO_2.[9]

The angular dependence of ionization can also be extracted from high harmonic generation (HHG) data. The amplitudes of the harmonics in HHG spectra of aligned molecules depend on the angle of the molecule relative to the laser field. Orbital tomography[10] can be used to reconstruct the shape of the highest occupied molecular orbital (HOMO) based on the three step model[11,12] and the SAE approximation. However, the simple orbital picture of HHG spectra remains under discussion.[13] Beyond the SAE approximation, orbital tomography can be interpreted as probing the Dyson orbitals plus exchange terms.[14] At higher intensities, angle-dependent ionization yields and HHG spectra also have contributions from lower lying orbitals.[15−28] These features appear to be the result of direct ionization from lower lying orbitals rather than excitation of the ion after ionization from the HOMO. Angle-dependent and channel-dependent ionization has also been measured in butadiene[29,30] and larger polyatomics.[31]

Molecular ADK theory[32] often provides a good description of ionization in the tunneling regime. The angular dependence of ionization can also be discussed in terms of the Dyson orbitals, which are computed from the overlap between the neutral and the ionic wave functions $\Phi_i^D = \int \Psi^{\text{neutral}} \Psi_i^{\text{cation}} d\tau_2 \ldots d\tau_n$. More quantitative descriptions of HHG and the angular dependence of ionization have been obtained by solving the time-dependent Schrödinger equation (TDSE) with more elaborate approaches such as quantitative rescattering theory,[33] time-dependent resolution-in-ionic-states,[17] SAE-TDSE,[9] time-dependent analytical R-matrix,[25] and time-dependent generalized active space configuration interaction.[34]

In the present study, we have examined the angle-dependence of strong-field ionization for O_2, N_2, CO_2, and CH_2O using a time-dependent configuration interaction (TDCI) approach. Response properties can be described well with TDCI methods using atom-centered basis functions.[35−39] Ionization by intense laser pulses can be simulated by including a complex absorbing potential (CAP).[40,41] Intense fields distort the wave function toward the CAP leading to absorption of a fraction of the wave function (to ensure sufficient interaction with the CAP, several sets of diffuse functions need to be added to the basis set). The ionization yield is obtained from the loss of norm of the wave function. The TDCI-CAP approach has been compared to accurate grid-based calculations, and yields good agreement for the ionization of H atom as a function of field strength, and the change in the rate of ionization of H_2^+ as a function of bond length.[40] The methodology has been used to study the ionization of ethylene, butadiene, and hexatriene as a function of field strength.[41] By calculating the variation of the ionization yield with the direction of polarization of the laser pulse, we can obtain the three-dimensional surfaces shown in Figures 1−4, which we interpret as angle-dependent ionization probabilities. The three-dimensional shapes of the ionization probabilities and their variation with the intensity of the laser pulses can be discussed in terms of ionization from the HOMO

Received: May 5, 2015
Accepted: May 25, 2015
Published: May 26, 2015

DOI: 10.1021/acs.jpclett.5b00929
J. Phys. Chem. Lett. 2015, 6, 2140−2146

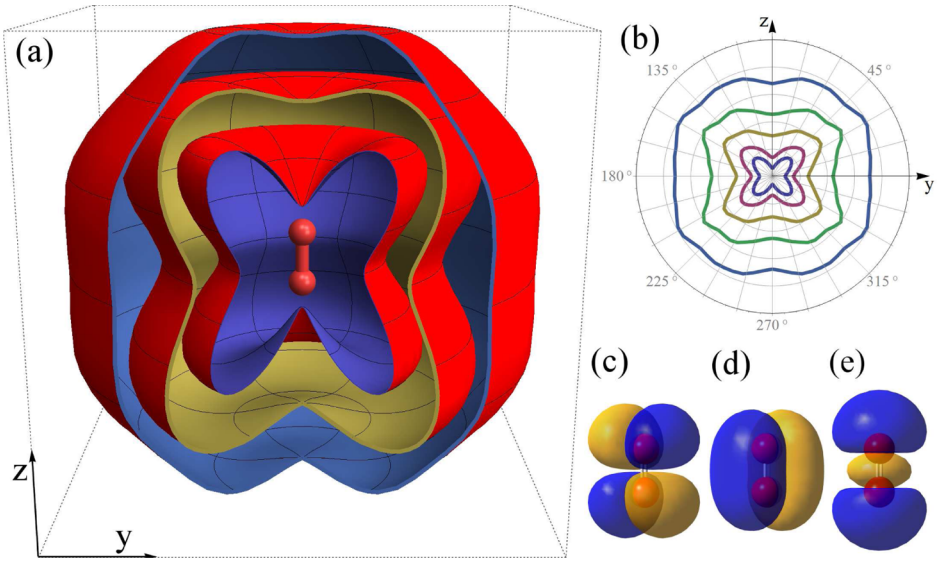

Figure 1. Angle dependence of the ionization yield for O_2 calculated with the TDCIS(D)-CAP approach: (a) three-dimensional plot for field strengths of 0.08, 0.10, 0.12 E_h/ea_0, (b) polar plot containing the molecular axis for field strengths of 0.08, 0.09, 0.10, 0.11, 0.12 E_h/ea_0, (c) the Dyson orbital for the $X\ ^2\Pi_g$ state, (d) the Dyson orbital for the $A\ ^2\Pi_u$ state, and (e) the Dyson orbital for the $B\ ^2\Sigma_g$ state.

and lower lying orbitals and the Dyson orbitals for the ground state and excited states of the cations.

The ionization dynamics are simulated by solving the time-dependent Schrödinger equation for the electronic wave function:

$$i\frac{\partial}{\partial t}\Psi_{el}(t) = [\hat{\mathbf{H}}_{el} - \hat{\vec{\mu}}\vec{E}(t) - i\hat{\mathbf{V}}^{Absorb}]\Psi_{el}(t) \tag{1}$$

where the total Hamiltonian includes the field-free electronic Hamiltonian, $\hat{\mathbf{H}}_{el}$, and the electron-light interaction, $\hat{\vec{\mu}}\vec{E}(t)$, treated in the semiclassical dipole approximation as a product of dipole operator and electric field component of the laser pulse. Ionization is modeled by including a CAP, $-i\hat{\mathbf{V}}^{Absorb}$. In the present work, V^{Absorb} has a quadratic rise and a quadratic turn over to a constant value of 10 E_h at long-range. V^{Absorb} is constructed from a set of overlapping spherical potentials around each atom at a distance of 3.5 times the van der Waals radius of each element (r_H = 5.051 Å for H, r_C = 6.739 Å for C, r_N = 6.405 Å for N, and r_O = 6.125 Å for O; see ref 40 for details of the form of the CAP and testing of the methodology). The size and shape of the absorbing potential for CO_2 can be seen in Figure 3b. The radii are chosen as a compromise between minimal absorption of the norm in the field-free case and the number of diffuse basis functions needed for interaction with the CAP.

The time-dependent wave function is expanded in the basis of the Hartree−Fock ground state and all singly excited states of the field-free, time-independent Hamiltonian:

$$\Psi(t) = \sum_{i=0} C_i(t)|\Psi_i\rangle \tag{2}$$

The coefficients are propagated using a Trotter factorization of the exponential of the Hamiltonian with a time step of Δt = 0.05 $\hbar/E_h$(1.2 as):

$$\begin{aligned}\Psi(t+\Delta t) &= \exp(-i\hat{\mathbf{H}}\Delta t)\Psi(t)\\ &= \exp(-i\mathbf{H}_{el}\Delta t/2)\exp(\mathbf{V}\Delta t/2)\mathbf{W}^T\\ &\quad\times\exp(iE(t+\Delta t/2)\mathbf{d}\Delta t)\mathbf{W}\exp(\mathbf{V}\Delta t/2)\\ &\quad\times\exp(-i\mathbf{H}_{el}\Delta t/2)\Psi(t)\end{aligned} \tag{3}$$

where $\mathbf{WDW}^T = \mathbf{d}$ are the eigenvalues and eigenvectors of the transition dipole matrix in the direction of the polarization of the laser field. $\mathbf{W}$, $\mathbf{d}$, $\exp(-i\hat{\mathbf{H}}\Delta t)$, and $\exp(\mathbf{V}\Delta t/2)$ need to be calculated only once, and the propagation involves a pair of matrix-vector multiplies and the exponential of the diagonal matrix, $\mathbf{d}$.

The energies of the field-free states for CO_2 and CH_2O were calculated with the CIS[42] method, while energies of the field-free states of O_2 and N_2 were calculated with the CIS(D)[43] method since this produced a better ordering for the excited states of the ions. More accurate methods for calculating the field free states would be desirable, but it is currently not practical to use methods such as EOMCC or MRCI to calculate the thousands of excited states and associated transition dipole and absorbing matrix elements needed for the TDCI method. The electronic structure calculations were carried out with a locally modified version of the *GAUSSIAN* program package[44] (the same matrix elements are used for CIS and CIS(D)). Spin unrestricted Hartree−Fock was used for triplet O_2, while spin restricted Hartree−Fock was used for N_2, CO_2, and CH_2O. The calculations employed the standard Dunning aug-cc-pVTZ basis set[45,46] augmented with an absorbing basis (AB) containing extra diffuse functions to ensure sufficient interaction with the CAP. This absorbing basis consists of nine sets of diffuse Gaussian functions on each atom: three *s* functions (with exponents: 0.0256, 0.0128, and 0.0064), two sets of *p* functions (0.0256, 0.0128), three sets of pure *d* functions (0.0512, 0.0256, and 0.0128), and one set of pure *f* functions (0.0256), (for details of the development of the absorbing basis, see refs 40 and 41). The molecules were aligned with the *z* axis and have the following geometries: 1.160 Å for O_2, and 1.067 Å for N_2, R(CO) = 1.136 Å for CO_2, and R(CO) = 1.179 Å, R(CH) = 1.092 Å, and ∠(CHO) = 121.947°

DOI: 10.1021/acs.jpclett.5b00929
J. Phys. Chem. Lett. 2015, 6, 2140−2146

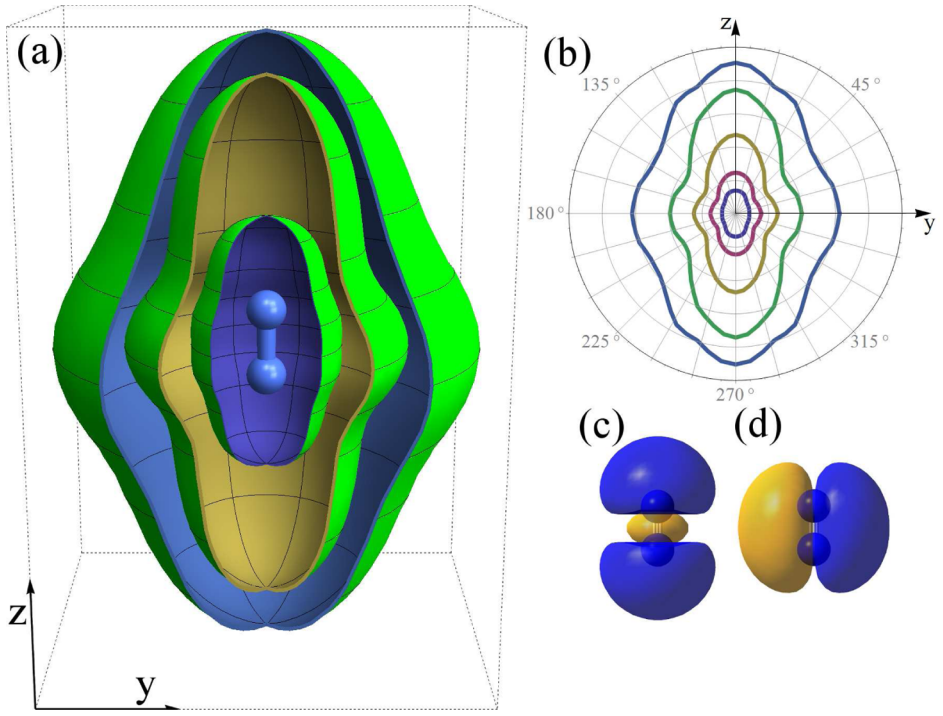

Figure 2. Angle dependence of the ionization yield for N_2 calculated with the TDCIS(D)-CAP approach. (a) three-dimensional plot for field strengths of 0.08, 0.10, 0.12 E_h/ea_0, (b) polar plot containing the molecular axis for field strengths of 0.08, 0.09, 0.10, 0.11, 0.12 E_h/ea_0, (c) the Dyson orbital for the $X\ ^2\Sigma_g$ state, (d) the Dyson orbital for the $A\ ^2\Pi_u$ state.

for CH_2O. Dyson orbitals were obtained from the overlap of the ground state of the neutral and the ground and excited states of the cation computed using single determinant Hartree−Fock calculations at the same geometry (since the orbitals of the neutral and the cation are different, this involves the overlap between nonorthogonal determinants). The ground state and all singly excited electronic states were used in the time-dependent configuration interaction calculations: 1703 states for O_2, 706 for N_2, 1633 for CO_2, and 1369 for CH_2O.

In this work, we apply linearly polarized cosine squared pulses with frequency of 0.057 $E_h/\hbar$(800 nm) and 7 optical cycles (9.35 fs fwhm), and propagate the system for a total of 1000 $\hbar/E_h$(24.2 fs). The maximal field strengths range from E_{max} = 0.04 $E_h/(ea_0)$ to 0.12 $E_h/(ea_0)$ correspond to peak intensities of 5.62×10^{13} and 5.05×10^{14} W/cm^2. For the molecules considered, ionization at these field strengths occurs primarily by barrier suppression rather than tunneling. The loss of norm was calculated after the pulse (18.7 fs) when the field has returned to zero and is taken as the ionization yield for the pulse. By varying the polarization direction of the pulse with a given E_{max}, we obtain a three-dimensional surface, which we interpret as an angle-dependent ionization probability. For each E_{max}, up to 114 points were calculated and a three-dimensional plot was generated using the ionization rate as the radial distance and the direction of the polarization as the angles. To obtain a smooth surface, the ionization rate as a function of the angles was fitted to a polynomial in $\cos(\theta)^n \cos(m\phi)$ and $\cos(\theta)^n \sin(m\phi)$, n = 0−9, m = 0−4.

Figures 1−4 show the total ionization rates as a function of the orientation of the laser field polarization. For a particular maximum field strength, the ionization yield is plotted as a distance from the origin as a function of the angle of the laser polarization. So that the angular dependence is easier to see in the three-dimensional plots, the ionization yield is scaled by a factor of 3 for the lowest intensity and by a factor of 1.5 for the second lowest intensity. Also included in the figures are more conventional polar plots of the angle dependent ionization rates (without scaling). The relevant Dyson orbitals are included in the figures to aid in the interpretation of the angular dependence of the ionization rate. The Dyson orbitals for the ground state and lowest two excited states of the cations closely resemble the canonical Hartree−Fock orbitals and have norms greater than 0.95 (the exceptions are 0.93 for π_g of CO_2 and 0.94 for a_1 of CH_2O).

For O_2, the angle-dependent ionization yield is shown in Figure 1a,b. For the $^2\Pi_g$ ground state of O_2^+, the Dyson orbital is a π_g antibonding orbital, shown in Figure 1c. At lower intensities, the angle-dependent ionization closely reflects the shape of the Dyson orbital. The ionization rate is lowest along the molecular axis, reaches a maximum around 45° and 135°, and decreases to a minimum at 90°, where the π_g orbital has a node. At higher intensities, the angular dependence of the ionization shows contributions from the σ_g orbital along the molecular axis and the π_u orbital perpendicular to the axis. The lowest excited states of O_2^+ are of $^2\Pi_u$ and $^2\Sigma_g$ symmetry and are associated with the π_u and σ_g Dyson orbitals. These excited states are 4−8 eV higher than the ground state of the ion.[47] Calculations of HHG spectra indicate that harmonic yields from the π_u and σ_g orbitals increase with increasing intensity.[27]

The angular dependence of the ionization yield for N_2 shown in Figure 2a,b appears to be a mixture of two contributions even at the lowest intensities. The large ionization rate along the molecular axis is associated with the $X\ ^2\Sigma_g$ state of N_2^+ and the loss of an electron from the σ_g lone pair orbital (Figure 2c). The increased ionization rate perpendicular to the molecular axis corresponds to the $A^2\Pi_u$ state of N_2^+ and loss of an electron from the π_u Dyson orbital (Figure 2d). Experimentally, the $A^2\Pi_u$ state is only 1.1 eV above the ground state and

DOI: 10.1021/acs.jpclett.5b00929
J. Phys. Chem. Lett. 2015, 6, 2140−2146

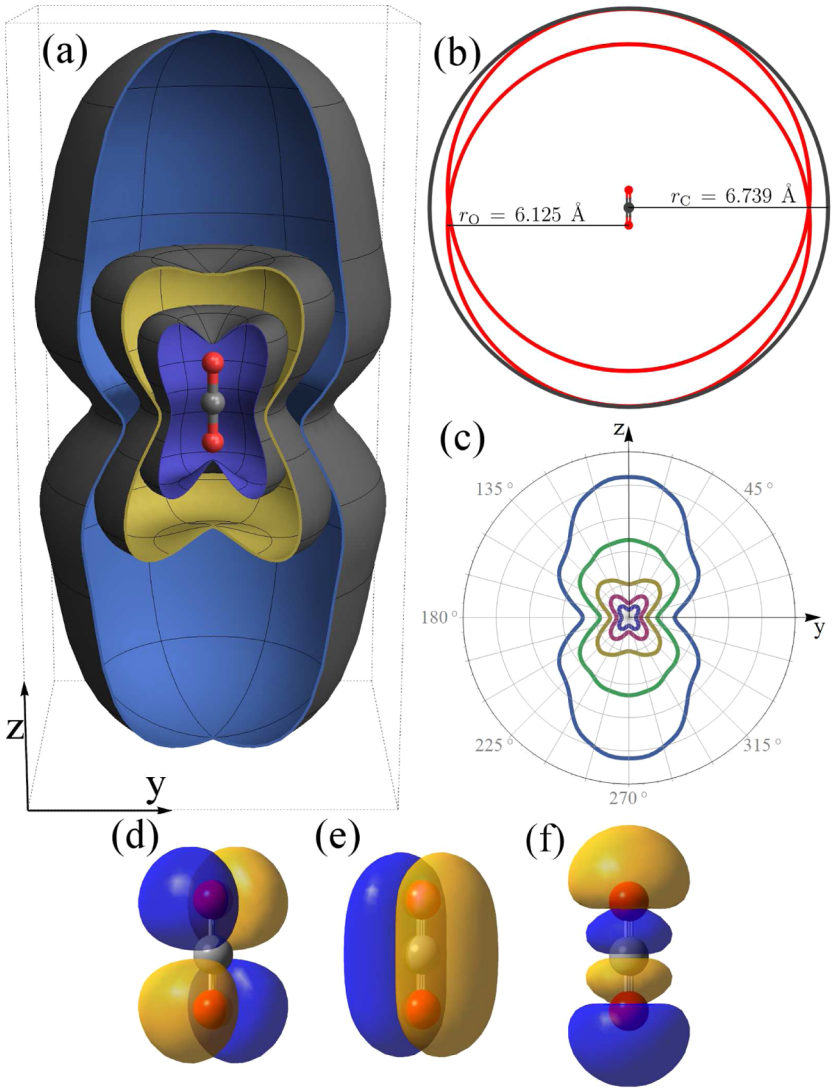

Figure 3. Angle dependence of the ionization yield for CO_2 calculated with the TDCIS-CAP approach: (a) three-dimensional plot for field strengths of 0.08, 0.10, 0.12 E_h/ea_0, (b) the CAP, (c) polar plot containing the molecular axis for field strengths of 0.08, 0.09, 0.10, 0.11, 0.12 E_h/ea_0, (d) the Dyson orbital for the $X\ ^2\Pi_g$ state, (e) the Dyson orbital for the $A\ ^2\Pi_u$ state, and (f) the Dyson orbital for the $B\ ^2\Sigma_u$ state.

participates in strong field ionization at higher intensities.[48] The experimental HHG spectra of N_2 are dominated by the σ_g orbital, but contributions from the π_u orbital can be seen in the HHG data.[15] The π_u contributions to the HHG spectra and the angle-dependent ionization grow with increasing laser intensity.[18,21] Orbital tomography has been used to reconstruct both the σ_g and the π_u orbitals from the real and imaginary parts of the emission dipole from coherent soft X-ray emission spectra.[23] SAE-TDSE calculations based on Kohn−Sham orbitals show that the σ_g orbital dominates ionization at all angles but the π_u orbital makes a significant contribution perpendicular to the molecular axis.[9]

Figure 3a,c shows the calculated angular dependence of the ionization rate for CO_2. At low values of E_{max}, the shape reflects the π_g Dyson orbital for ground state CO_2^+, as depicted in Figure 3d. The ionization yield shows a broad maximum around 50° and minima along the molecular axis and perpendicular to the axis. The experimental angular dependence of the ionization has a maximum at 45°.[7,8] Molecular ADK theory has a sharp maximum at 25°,[7] but more careful application of MO-ADK[19] and more elaborate theories have broader maxima in the 30−45° range.[9,17,20,25,28] At higher E_{max}, there is a large increase in the ionization rate along the molecular axis. This is indicative of ionization to the $B\ ^2\Sigma_u$ state of CO_2^+ and the Dyson orbital corresponds to the σ_u orbital involving the oxygen lone pairs, Figure 3f. Ionization from the Dyson orbital for the $A\ ^2\Pi_u$ state, Figure 3e, does not seem to contribute to the angular dependence. The $^2\Pi_u$ and $^2\Sigma_u$ state of CO_2^+ are 3.5 and 4.3 eV higher than the ground state, respectively.[47] Fluorescence spectra indicate that strong field ionization produces the $A\ ^2\Pi_u$ and $B\ ^2\Sigma_u$ states of CO_2^+ as well as the ground state.[24] Analysis of HHG spectra of CO_2^+ reveal contributions from ionization from lower lying orbitals.[16,22] Calculations by other groups also show that the σ_u orbital contributes to ionization along the molecular axis and the π_u orbital contributes to ionization perpendicular to the axis,[9,25,28] and that at higher intensities these contributions can become larger than from the π_g orbital.[28]

The angular dependence of the ionization of formaldehyde (Figure 4a−c) has a richer three-dimensional structure since it lacks the cylindrical symmetry of linear molecules in this study. The Dyson orbital for the ground state of CH_2O^+ is an

DOI: 10.1021/acs.jpclett.5b00929
J. Phys. Chem. Lett. 2015, 6, 2140−2146

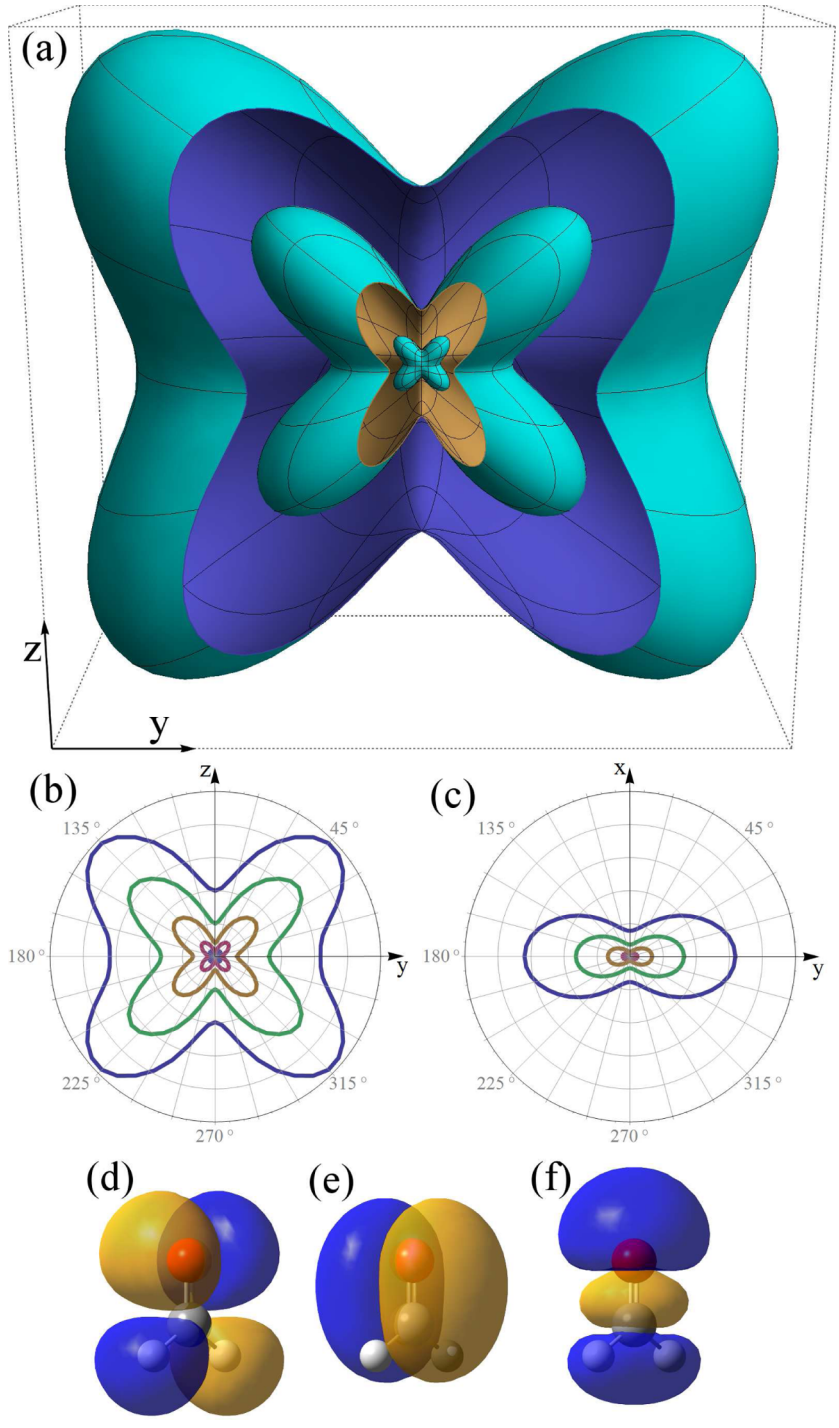

Figure 4. Angle dependence of the ionization yield for CH_2O calculated with the TDCIS-CAP approach: (a) three-dimensional plot for field strengths of 0.04, 0.06, 0.08 E_h/ea_0, (b) polar plot containing the molecular axis for field strengths of 0.04, 0.05, 0.06, 0.07, 0.08 E_h/ea_0, (c) polar plot perpendicular the molecular axis, (d) the Dyson orbital for the $^2B_2$ state, (e) the Dyson orbital for the $^2B_1$ state, and (f) the Dyson orbital for the $^2A_1$ state.

antibonding combination of the in-plane *p*-type lone pair on oxygen and the antisymmetric combination of the C−H bonds. The shape of the ionization probability as well as the polar plot of the in-plane ionization rate corresponds closely to this b_2 Dyson orbital. The lowest two excited states of CH_2O^+ have a Dyson orbital with b_1 (π_g) and a_1 (σ) symmetry and are about 3.2 and 5.4 eV higher in energy, respectively. Some evidence of ionization from the a_1 orbital is seen at higher values of E_{max} than shown in the plots. Experimental studies of the angular dependence of ionization have not yet been reported for formaldehyde. HHG and strong field ionization of CH_2O have been studied by grid-based time-dependent density functional simulations.[49] For laser polarizations aligned with the CO bond and perpendicular to the molecular plane, the response is dominated by ionization from the b_2 orbital with some contribution from the a_1 orbital but little from the b_1 orbital. With increasing intensity, ionization increases significantly for the b_2 and a_1 orbitals, but not for the b_1 orbital.

DOI: 10.1021/acs.jpclett.5b00929
J. Phys. Chem. Lett. 2015, 6, 2140−2146

In this paper we have demonstrated the use of the TDCI-CAP approach to simulate the angular dependence of ionization of O_2, N_2, CO_2, and CH_2O. At low intensities, the angular dependence is dominated by the shape of the Dyson orbital associated with the ground state of the ion. At higher intensities, the calculated angular distributions show contributions from ionization of lower lying orbitals. The TDCI-CAP approach is readily scalable to larger polyatomic systems (unpublished results).

AUTHOR INFORMATION

Corresponding Author

*E-mail: hbs@chem.wayne.edu.

Notes

The authors declare no competing financial interest.

ACKNOWLEDGMENTS

This work was supported by a grant from the National Science Foundation (CHE1212281, CHE1464450). We thank Wayne State University's computing grid for computer time.

REFERENCES

(1) Kling, M. F.; Vrakking, M. J. Attosecond Electron Dynamics. *Annu. Rev. Phys. Chem.* **2008**, *59*, 463−492.

(2) Krausz, F.; Ivanov, M. Attosecond Physics. *Rev. Mod. Phys.* **2009**, *81*, 163−234.

(3) Gallmann, L.; Cirelli, C.; Keller, U. Attosecond Science: Recent Highlights and Future Trends. *Annu. Rev. Phys. Chem.* **2012**, *63*, 447−469.

(4) Litvinyuk, I. V.; Lee, K. F.; Dooley, P. W.; Rayner, D. M.; Villeneuve, D. M.; Corkum, P. B. Alignment-Dependent Strong Field Ionization of Molecules. *Phys. Rev. Lett.* **2003**, *90*, 233003.

(5) Pinkham, D.; Jones, R. R. Intense Laser Ionization of Transiently Aligned CO. *Phys. Rev. A* **2005**, *72*, 023418.

(6) Alnaser, A. S.; Voss, S.; Tong, X. M.; Maharjan, C. M.; Ranitovic, P.; Ulrich, B.; Osipov, T.; Shan, B.; Chang, Z.; Cocke, C. L. Effects of Molecular Structure on Ion Disintegration Patterns in Ionization of O_2 and N_2 by Short Laser Pulses. *Phys. Rev. Lett.* **2004**, *93*, 113003.

(7) Pavičić, D.; Lee, K. F.; Rayner, D. M.; Corkum, P. B.; Villeneuve, D. M. Direct Measurement of the Angular Dependence of Ionization for N_2, O_2, and CO_2 in Intense Laser Fields. *Phys. Rev. Lett.* **2007**, *98*, 243001.

(8) Thomann, I.; Lock, R.; Sharma, V.; Gagnon, E.; Pratt, S. T.; Kapteyn, H. C.; Murnane, M. M.; Li, W. Direct Measurement of the Angular Dependence of the Single-Photon Ionization of Aligned N_2 and CO_2^+. *J. Phys. Chem. A* **2008**, *112*, 9382−9386.

(9) Petretti, S.; Vanne, Y. V.; Saenz, A.; Castro, A.; Decleva, P. Alignment-Dependent Ionization of N_2, O_2, and CO_2 in Intense Laser Fields. *Phys. Rev. Lett.* **2010**, *104*, 223001.

(10) Itatani, J.; Levesque, J.; Zeidler, D.; Niikura, H.; Pépin, H.; Kieffer, J. C.; Corkum, P. B.; Villeneuve, D. M. Tomographic Imaging of Molecular Orbitals. *Nature* **2004**, *432*, 867−871.

(11) Corkum, P. B. Plasma Perspective on Strong Field Multiphoton Ionization. *Phys. Rev. Lett.* **1993**, *71*, 1994−1997.

(12) Lewenstein, M.; Balcou, P.; Ivanov, M. Y.; L'Huillier, A.; Corkum, P. B. Theory of High-Harmonic Generation by Low-Frequency Laser Fields. *Phys. Rev. A* **1994**, *49*, 2117−2132.

(13) Schwarz, W. H. E. Measuring Orbitals: Provocation or Reality? *Angew. Chem., Int. Ed.* **2006**, *45*, 1508−1517.

(14) Patchkovskii, S.; Zhao, Z.; Brabec, T.; Villeneuve, D. M. High Harmonic Generation and Molecular Orbital Tomography in Multielectron Systems: Beyond the Single Active Electron Approximation. *Phys. Rev. Lett.* **2006**, *97*, 123003.

(15) McFarland, B. K.; Farrell, J. P.; Bucksbaum, P. H.; Gühr, M. High Harmonic Generation from Multiple Orbitals in N_2. *Science* **2008**, *322*, 1232−1235.

(16) Smirnova, O.; Mairesse, Y.; Patchkovskii, S.; Dudovich, N.; Villeneuve, D.; Corkum, P.; Ivanov, M. Y. High Harmonic Interferometry of Multi-Electron Dynamics in Molecules. *Nature* **2009**, *460*, 972−977.

(17) Spanner, M.; Patchkovskii, S. One-electron Ionization of Multielectron Systems in Strong Nonresonant Laser Fields. *Phys. Rev. A* **2009**, *80*, 063411.

(18) Son, S.-K.; Chu, S.-I. Theoretical Study of Orientation-Dependent Multiphoton Ionization of Polyatomic Molecules in Intense Ultrashort Laser Fields: A New Time-Dependent Voronoi-Cell Finite Difference Method. *Chem. Phys.* **2009**, *366*, 91−102.

(19) Zhao, S.-F.; Jin, C.; Le, A.-T.; Jiang, T. F.; Lin, C. D. Analysis of Angular Dependence of Strong-Field Tunneling Ionization for CO_2. *Phys. Rev. A* **2009**, *80*, 051402.

(20) Son, S.-K.; Chu, S.-I. Multielectron Effects on the Orientation Dependence and Photoelectron Angular Distribution of Multiphoton Ionization of CO_2 in Strong Laser Fields. *Phys. Rev. A* **2009**, *80*, 011403.

(21) Le, A.-T.; Lucchese, R. R.; Lin, C. D. Uncovering multiple Orbitals Influence in High Harmonic Generation from Aligned N_2. *J. Phys. B* **2009**, *42*, 211001.

(22) Smirnova, O.; Patchkovskii, S.; Mairesse, Y.; Dudovich, N.; Ivanov, M. Y. Strong-Field Control and Spectroscopy of Attosecond Electron-Hole Dynamics in Molecules. *Proc. Natl. Acad. Sci. U. S. A.* **2009**, *106*, 16556−16561.

(23) Haessler, S.; Caillat, J.; Boutu, W.; Giovanetti-Teixeira, C.; Ruchon, T.; Auguste, T.; Diveki, Z.; Breger, P.; Maquet, A.; Carré, B.; et al. Attosecond Imaging of Molecular Electronic Wavepackets. *Nat. Phys.* **2010**, *6*, 200−206.

(24) Wu, C.; Zhang, H.; Yang, H.; Gong, Q.; Song, D.; Su, H. Tunneling Ionization of Carbon Dioxide from Lower-Lying Orbitals. *Phys. Rev. A* **2011**, *83*, 033410.

(25) Torlina, L.; Ivanov, M.; Walters, Z. B.; Smirnova, O. Time-Dependent Analytical *R*-Matrix Approach for Strong-Field Dynamics. II. Many-Electron Systems. *Phys. Rev. A* **2012**, *86*, 043409.

(26) Jin, C.; Bertrand, J. B.; Lucchese, R. R.; Wörner, H. J.; Corkum, P. B.; Villeneuve, D. M.; Le, A.-T.; Lin, C. D. Intensity Dependence of Multiple Orbital Contributions and Shape Resonance in High-Order Harmonic Generation of Aligned N_2 Molecules. *Phys. Rev. A* **2012**, *85*, 013405.

(27) Zhang, J.; Wu, Y.; Zeng, Z.; Xu, Z. Intensity-Dependent Multiorbital Effect in High-Order Harmonics Generated from Aligned O_2 Molecules. *Phys. Rev. A* **2013**, *88*, 033826.

(28) Li, J.; Liu, P.; Yang, H.; Song, L.; Zhao, S.; Lu, H.; Li, R.; Xu, Z. High Harmonic Spectra Contributed by HOMO-1 Orbital of Aligned CO_2 Molecules. *Opt. Express* **2013**, *21*, 7599−7607.

(29) Boguslavskiy, A. E.; Mikosch, J.; Gijsbertsen, A.; Spanner, M.; Patchkovskii, S.; Gador, N.; Vrakking, M. J. J.; Stolow, A. The Multielectron Ionization Dynamics Underlying Attosecond Strong-Field Spectroscopies. *Science* **2012**, *335*, 1336−1340.

(30) Mikosch, J.; Boguslavskiy, A. E.; Wilkinson, I.; Spanner, M.; Patchkovskii, S.; Stolow, A. Channel- and Angle-Resolved Above Threshold Ionization in the Molecular Frame. *Phys. Rev. Lett.* **2013**, *110*, 023004.

(31) Njoya, O.; Matsika, S.; Weinacht, T. Angle-Resolved Strong-Field Ionization of Polyatomic Molecules: More than the Orbitals Matters. *ChemPhysChem* **2013**, *14*, 1451−1455.

(32) Tong, X. M.; Zhao, Z. X.; Lin, C. D. Theory of Molecular Tunneling Ionization. *Phys. Rev. A* **2002**, *66*, 033402.

(33) Le, A.-T.; Lucchese, R. R.; Tonzani, S.; Morishita, T.; Lin, C. D. Quantitative Rescattering Theory for High-Order Harmonic Generation from Molecules. *Phys. Rev. A* **2009**, *80*, 013401.

(34) Bauch, S.; Sørensen, L. K.; Madsen, L. B. Time-Dependent Generalized-Active-Space Configuration-Interaction Approach to Photoionization Dynamics of Atoms and Molecules. *Phys. Rev. A* **2014**, *90*, 062508.

(35) Schlegel, H. B.; Smith, S. M.; Li, X. Electronic Optical Response of Molecules in Intense Fields: Comparison of TD-HF, TD-CIS, and TD-CIS(D) Approaches. *J. Chem. Phys.* **2007**, *126*, 244110.

DOI: 10.1021/acs.jpclett.5b00929
J. Phys. Chem. Lett. 2015, 6, 2140−2146

(36) Krause, P.; Klamroth, T.; Saalfrank, P. Molecular Response Properties from Explicitly Time-Dependent Configuration Interaction Methods. *J. Chem. Phys.* **2007**, *127*, 034107.
(37) Breidbach, J.; Cederbaum, L. S. Migration of Holes: Numerical Algorithms and Implementation. *J. Chem. Phys.* **2007**, *126*, 034101.
(38) Mignolet, B.; Levine, R. D.; Remacle, F. Localized Electron Dynamics in Attosecond-Pulse-Excited Molecular Systems: Probing the Time-Dependent Electron Density by Sudden Photoionization. *Phys. Rev. A* **2012**, *86*, 053429.
(39) Luppi, E.; Head-Gordon, M. The Role of Rydberg and Continuum Levels in Computing High Harmonic Generation Spectra of the Hydrogen Atom Using Time-Dependent Configuration Interaction. *J. Chem. Phys.* **2013**, *139*, 164121.
(40) Krause, P.; Sonk, J.; Schlegel, H. B. Strong Field Ionization Rates Simulated with Time-Dependent Configuration Interaction and an Absorbing Potential. *J. Chem. Phys.* **2014**, *140*, 174113.
(41) Krause, P.; Schlegel, H. B. Strong-Field Fonization Rates of Linear Polyenes Simulated with Time-Dependent Configuration Interaction with an Absorbing Potential. *J. Chem. Phys.* **2014**, *141*, 174104.
(42) Foresman, J. B.; Head-Gordon, M.; Pople, J. A.; Frisch, M. J. Toward a Systematic Molecular Orbital Theory for Excited States. *J. Phys. Chem.* **1992**, *96*, 135−149.
(43) Head-Gordon, M.; Rico, R. J.; Oumi, M.; Lee, T. J. A Doubles Correction to Electronic Excited States from Configuration Interaction in the Space of Single Substitutions. *Chem. Phys. Lett.* **1994**, *219*, 21−29.
(44) Frisch, M. J.; Trucks, G. W.; Schlegel, H. B.; Scuseria, G. E.; Robb, M. A.; Cheeseman, J. R.; Scalmani, G.; Barone, V.; Mennucci, B.; Petersson, G. A.et al. *Gaussian Development Version*, revision H.20+; Gaussian, Inc: Wallingford, CT, 2010.
(45) Dunning, T. H., Jr. Gaussian Basis Sets for Use in Correlated Molecular Calculations. I. The Atoms Boron Through Neon and Hydrogen. *J. Chem. Phys.* **1989**, *90*, 1007−1023.
(46) Wilson, A. K.; van Mourik, T.; Dunning, T. H., Jr. Gaussian Basis Sets for Use in Correlated Molecular Calculations. VI. Sextuple Zeta Correlation Consistent Basis Sets for Boron Through Neon. *J. Mol. Struct.: THEOCHEM* **1996**, *388*, 339−349.
(47) Rosenstock, H. M.; Draxl, K.; Steiner, B. W.; Herron, J. T. Energies of Gaseous Ions. *J. Phys. Chem. Ref. Data* **1997**, *6 Suppl. 1*, 1−783.
(48) Becker, A.; Bandrauk, A.; Chin, S. S-Matrix Analysis of Non-Resonant Multiphoton Ionisation of Inner-Valence Electrons of the Nitrogen Molecule. *Chem. Phys. Lett.* **2001**, *343*, 345−350.
(49) Penka, E. F.; Couture-Bienvenue, E.; Bandrauk, A. D. Ionization and Harmonic Generation in CO and H_2CO and Their Cations with Ultrashort Intense Laser Pulses with Time-Dependent Density-Functional Theory. *Phys. Rev. A* **2014**, *89*, 023414.

DOI: 10.1021/acs.jpclett.5b00929
J. Phys. Chem. Lett. 2015, 6, 2140−2146